Chemical Engineering Journal 156 (2010) 546–552

Contents lists available at ScienceDirect

Chemical Engineering Journal

journal homepage: www.elsevier.com/locate/cej

Effects of surface free energy and nanostructures on dropwise condensation

Lan Zhong, Ma Xuehu*, Wang Sifang, Wang Mingzhe, Li Xiaonan

Institute of Chemical Engineering, Dalian University of Technology, Dalian 116012, China

ARTICLE INFO

Article history:
Received 25 October 2008
Received in revised form 2 April 2009
Accepted 2 April 2009

Keywords:
Dropwise condensation
Nanostructure
Surface free energy
Superhydophobicity
Self-assembled monolayers

ABSTRACT

Effects of surface free energy and nanostructures on dropwise condensation (DWC) were investigated experimentally. The oxidation and etching methods were applied to prepare the nanostructures on the copper substrates. Self-assembled monolayers coatings of *n*-octadecyl mercaptan were prepared on mirror-polished (SAM-2) and the nanostructured (SAM-1) copper substrates to promote the DWC. Experimental data presented that the nanostructure surface SAM-1 did not improve the dropwise condensation heat-transfer performance so much as to be expected for increasing the possible condensing surface area, compared to the mirror-polished SAM-2. This may be caused from the nanostructure's retardance to the condensate film. However, the incorporating effects of surface free energy and nanostructures of the condensing surface were found to play a really important role in the condensation heat-transfer enhancement. The fractal-like structures and the voids on SAM-1 surface were filled with condensate in the condensing process which resulted in a composite condensing surface of condensate and copper regions. Thus the average surface free energy of this composite condensing surface is larger than that of SAM-2 surface. The surface free energy difference between the condensate and the condensing surface of SAM-1 is less than that of SAM-2, so are the heat-transfer coefficients. The condensation heat-transfer is enhanced by a factor of 3 for SAM-2 surface, due to an increase of surface free energy difference between the condensate and condensing surface.

1. Introduction

Dropwise condensation (DWC) has been of considerable interests due to its higher heat-transfer coefficients than filmwise condensation (FWC) ever since discovered in 1930 [1–5]. The physical chemistry properties, such as surface free energy, roughness and surface topography, influence the configurations and motions of the condensate droplets directly [6–10]. Therefore, the heat-transfer characteristics during condensation varied with different surfaces. The low surface energy or the hydrophobic property of solid surface plays an important role in the dropwise condensation process. The surface wettability of solid surface was modified to realize the dropwise condensation [11]. Organic and polymer materials with low surface energy were used to promote DWC for their hydrophobic properties [12–17]. Das et al. [18] applied an organic self-assembled monolayers coating to enhance the dropwise condensation heat-transfer by a factor of 4. The lower the surface energy is, the higher the heat-transfer coefficient the dropwise condensation exhibits [19]. Ma et al. [20] proposed that the heat-transfer coefficient increases with the increase of the surface free energy difference between the condensate and the condensing surface. Lan [21] developed a heat-transfer model with consideration of the interfacial interaction between the condensate and the condensing surface. Neumann et al. [22] investigated the effect of the contact angle hysteresis on the heat-transfer characteristics during DWC. It was found that the heat-transfer during DWC is related to the contact angle hysteresis of the surface. The larger the contact angle hysteresis is, the lower the heat-transfer coefficient is. Superhydrophobic surfaces exhibit high contact angle (between 150° and 180°), low water contact angle hysteresis and low water roll-off angle [23–25]. Superhydrophobicity seems to likely promote dropwise condensation much more than other kind surfaces. Chen et al. [26] have recently reported continuous dropwise condensation on a superhydrophobic surface with short carbon nanotubes deposited on micromachined posts, a two-tier texture mimicking lotus leaves, superhydrophobicity is retained during and after condensation and rapid drop removal is enabled with a hexadecanethiol coating.

In this paper, a superhydrophobic surface prepared with self-assembled monolayers (SAM) coatings of *n*-octadecyl mercaptan on copper substrates with/without nanostructures was made to promote the DWC. The steam condensation experiments on a vertical plate were conducted to examine the heat-transfer characteristics. The effect of surface free energy and nanostructures on DWC was investigated.

* Corresponding author. Tel.: +86 411 83653402; fax: +86 411 83653402.
E-mail address: xuehuma@dlut.edu.cn (M. Xuehu).

1385-8947/$ – see front matter © 2009 Elsevier B.V. All rights reserved.
doi:10.1016/j.cej.2009.04.007

Nomenclature

f	fraction of solid surface area in contact with the water drop
h	condensation heat-transfer coefficient ($kW\,m^{-2}\,K^{-1}$)
P	pressure (kPa)
q	heat flux ($kW\,m^{-2}$)
SAM-1	*n*-octadecyl mercaptan SAM coated surface with nanostructures
SAM-2	*n*-octadecyl mercaptan SAM coated surface without nanostructures
T	temperature (K)
W	mole content of non-condensable gas in mixtures (%)
x	thermocouple position in condensing block (m)

Greek letters

λ	thermal conductivity ($W\,m^{-1}\,K^{-1}$)
θ	contact angle (°)

Subscripts

b	bulk
i	position of the thermocouples
s	solid phase or saturation
w	condensing wall
–	average value

2. Experimental apparatus

The condensation experiment schematic diagram is shown in Fig. 1. The experimental apparatus system is comprised of four parts: the boiler, cooling water, condensing chamber, and data acquisition and control system. The condensation chamber is made of stainless steel. Pressure were measured with a manometer with an uncertainty of ± 0.1% of the full scale (0–100 kPa), and the ambient pressure was determined with a standard mercury barometer. All copper-constantan thermocouples used in the experiments are calibrated in a high-precision constant-temperature bath against a standard platinum resistance thermometer calibrated by the National Metrical Laboratory of China.

A polynomial is fitted to the combined data for each thermocouple, compared to the standards platinum resistance thermometer the deviation of the calibrated T type thermocouple is within ± 0.1 K. Experimental measuring data are collected with the Agilent34970A data acquisition system, and all of the data including pressure, thermocouple readings, surface sub-cooling temperature, non-condensable gas (NCG) content, heat flux, heat-transfer coefficients can be calculated by instantaneous computation software, and the real-time data profiles can be displayed on a computer monitor. The linearity among the four readings from thermocouples embedded in the condensing block is checked by the instantaneous reduced data, only when the linearity is greater than 0.98, then, the experimental results are considered to be effective. All the experiments are operated at atmospheric pressure and repeated under the same operation conditions the other day.

Fig. 2 shows a schematic of the measurement system for the copper condensing block. A cylindrical condensing block, 30 mm in diameter and 410 mm long made from a high purity copper was thermally insulated with PTFE to ensure the one dimensional steady-state conduction. And the thermal conductivity of the copper block was assumed constant. Four holes with a 1 mm diameter were drilled into the block in parallel along the thermal stream; the type T copper-constantan thermocouple wires filled together with thermal compounds to ensure well contact between the thermocouple probe and the copper block were inserted into the bottom of each hole to measure the temperatures for each point. The cooling-side heat-transfer surface was extended with 15 rectangular fins to match the dropwise condensation heat-transfer capacity. Cooling water is supplied from a constant-temperature bath. The difference of the temperatures of the copper surface and the vapour is controlled by an electrical heater in the constant thermal water bath.

The whole system was pumped down to 0.1 kPa. After 24 h, the pressure was held 0.1 kPa with no leakage. Then the boiler was charged with deionized water and the air was removed out of the experimental system by a vacuum pump at the ambient temperature. Subsequently, the boiler was heated by two immersion

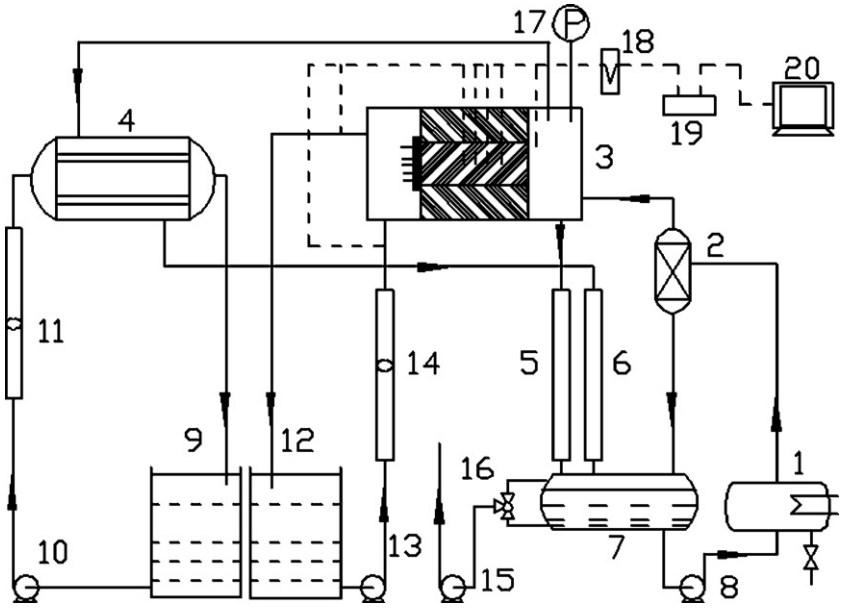

Fig. 1. Schematic diagram of the experimental system
1-boiler; 2-vapour-liuid separator; 3-condensation chamber; 4-secondary condenser; 5,6-measuring tube; 7-liquid tank; 8,10,13-pump; 9,12-coolent water; 11,14-flowmeter; 15-vacuum pump; 16-three-way valve; 17-pressure gauge; 18-ice-bottle; 19,20-data acquisition system.

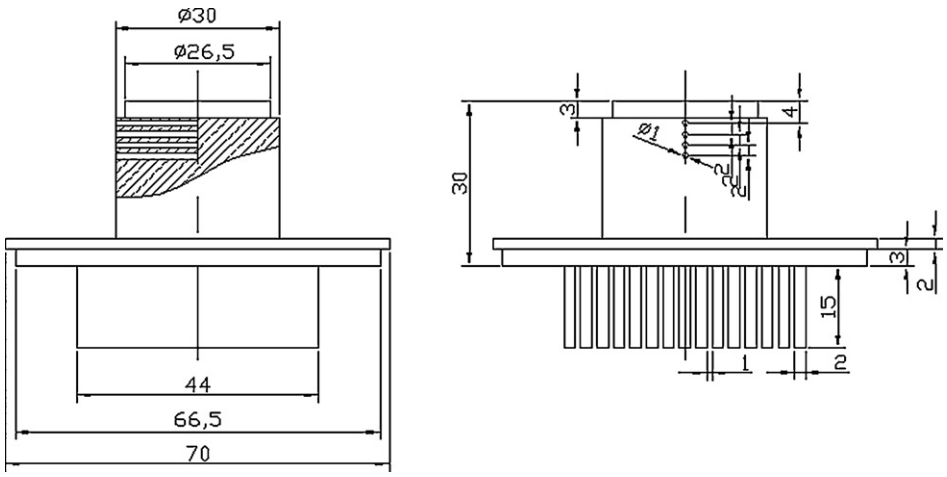

Fig. 2. Schematic diagram of the measurement system for the copper block condenser.

electrical heaters. When the water was heated up to the designed temperature and boiled for about 20 min, the vacuum pump was started again to remove the non-condensable gases in the experimental system. After a period of 10–15 min boiling, the system was pumped once again. The operation would be repeated for five times to remove the non-condensable gas both in the system and dissolved in water. After the appropriate degassing, the pumping line was closed.

3. Data reduction

Sixty values were collected for each point, and finally the average value was determined to obtain the heat flux and the wall temperature.

The heat flux, q, is determined using the least square method from the temperatures collected in the condensing block;

$$q = -\lambda_s \frac{\sum_{i=1}^{4}(x_i - \overline{x})(T_i - \overline{T})}{\sum_{i=1}^{4}(x_i - \overline{x})^2} \quad (1)$$

where,

$$\overline{T} = \frac{1}{4}(T_1 + T_2 + T_3 + T_4) \quad (2)$$

$$\overline{x} = \frac{1}{4}(x_1 + x_2 + x_3 + x_4) \quad (3)$$

A mean temperature of the condensing surface T_w was calculated by extrapolating the temperature gradient to the condensation surface

$$T_w = \overline{T} + \frac{q}{\lambda_s}\overline{x} \quad (4)$$

Therefore, the heat-transfer coefficient can be determined from the following relationships:

$$h = \frac{q}{\Delta T} = \frac{q}{T_b - T_w} \quad (5)$$

Non-condensable gas, mole fraction in the experimental system is calculated from the Gibbs-Dalton ideal gas mixture equation as shown in Eq. (6):

$$W = \frac{P_b - P_s(T_b)}{P_b} \quad (6)$$

The uncertainties of the measured and calculated parameters are estimated. The experimental uncertainties associated with the sensors and calculated parameters are as follows: temperature, ±0.05 K; pressure transducer 0.05 kPa; thermal driving force, $T_b - T_w$, ±2.4%; condensation heat-transfer coefficient, 5.7%; condensation heat flux ±2.1%; and the non-condensable gas content ±0.1%.

4. Self-assembled monolayers coatings

4.1. Formation of SAM coatings of n-octadecyl mercaptan on copper substrates

The *n*-octadecyl mercaptan was used as the DWC promoter. First, the surface of the copper condensing block was finely polished. For SAM-1, the copper substrate was immersed in a 30% hydrogen peroxide (H_2O_2) solution for 3.5 h, during which an oxide layer was formed on the copper surface. Then it was rinsed by deionized water, dried in the air and immersed in the 2.5 mmol/L solution of *n*-octadecyl mercaptan in ethanol for 1 h at 343 K. Thus, a SAM film of *n*-octadecyl mercaptan formed on the substrate. As the control group, SAM-2 was prepared in the same procedures without oxidation and etching process in H_2O_2 solution.

4.2. Contact angle measurement

Contact angles were measured to determine the hydrophobicity of the SAM coated surfaces, as shown in Fig. 3, by the sessile drop method using an OCA20 (Dataphysics Co., Germany) type contact angle measurement apparatus with an accuracy of ±0.1°. The contact angles of SAM-1 and SAM-2 are 165 ± 5° and 116 ± 5°, respectively.

4.3. SEM characterization and condensing surface configurations

The microstructures of the SAM surfaces were characterized by a scanning electron microscope (2800B, KYKY Tech Dev LTD, China.). Fig. 4 shows the SEM images of (a) finely polished copper surface, (b) SAM-2 surface, (c) nanostructured surface (copper substrate after oxidation and etching), (d) SAM-1 surface. As the SAM layer is very thin, the SAM coatings did not change the morphology of the copper substrates significantly. It can be seen from Fig. 4(c) that there were lots of fractal-like microstructures, voids and clusters on the copper substrate, due to the oxidation and etching treatment.

To fully interpret the superhydrophobicity of the surface, the contact angles can be expressed by the modified Cassie–Baxter

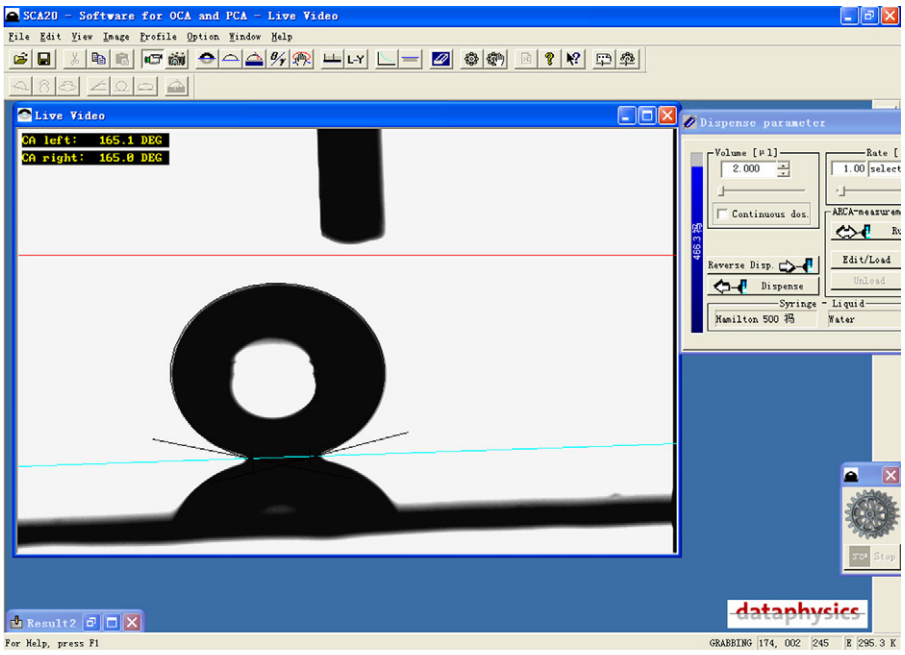

(a) Contact angle measurement for SAM-1 surface

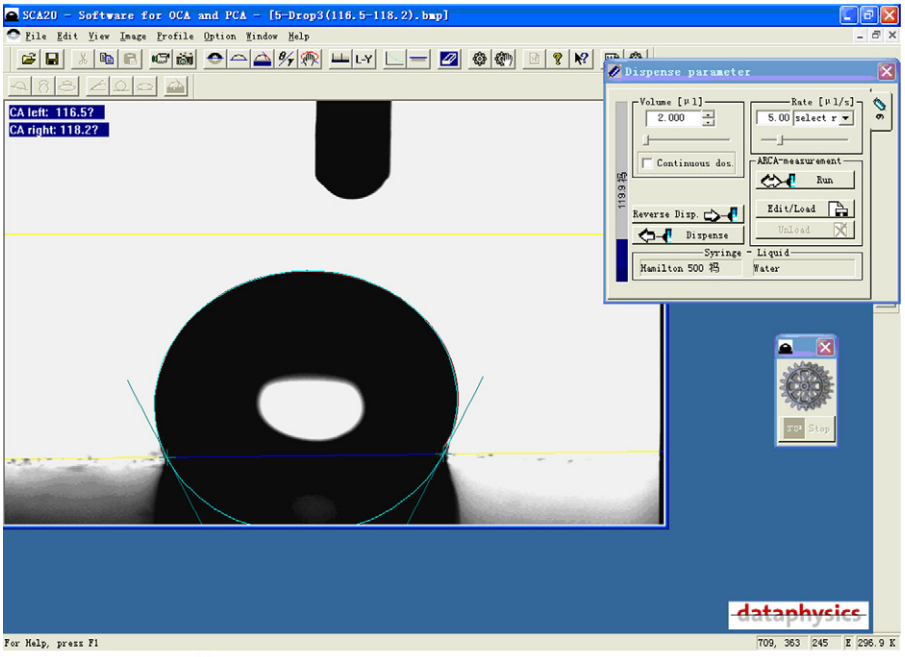

(b) Contact angle measurement for SAM-2 surface

Fig. 3. Contact angle measurements for (a) SAM-1 surface, (b) SAM-2 surface.

model [27] which predicts the equilibrium contact angle as

$$\cos\theta' = f(1+\cos\theta) - 1 \quad (6)$$

where, f is the fraction of solid surface area in contact with the water drop and remaining area $(1-f)$ is occupied by air for which the contact angle of water is 180°, θ is the contact angle on the corresponding smooth surface and θ' is the contact angle on the rough surface. With this model, it is possible to obtain $\theta' > 90°$ even if $\theta < 90°$, provided that f is very small, which can be achieved by means of hierarchical structures.

The fractions of solid surface, f, of the sample coated with SAM-1 was calculated with the measured contact angle θ' of 165°, and θ of 116° for the smooth surface. The calculated f value is found to be 0.06 for the microstructures. Consequently, air trapped in the cavities on rough surfaces results in a composite solid-air-liquid interface, substituting for the conventional solid–liquid homogeneous interface [28]. The surface energy of the composite surface is much lower.

5. Heat-transfer results

Both SAM-1 and SAM-2 coated surfaces have promoted the DWC as shown in Fig. 5. Fig. 6 shows the variations of heat fluxes with the vapour-surface temperature differences. Compared to the predicted value of Nusselt model of filmwise condensation, heat fluxes here were enhanced by a factor of 3 and 1.8 for SAM-2 and SAM-1

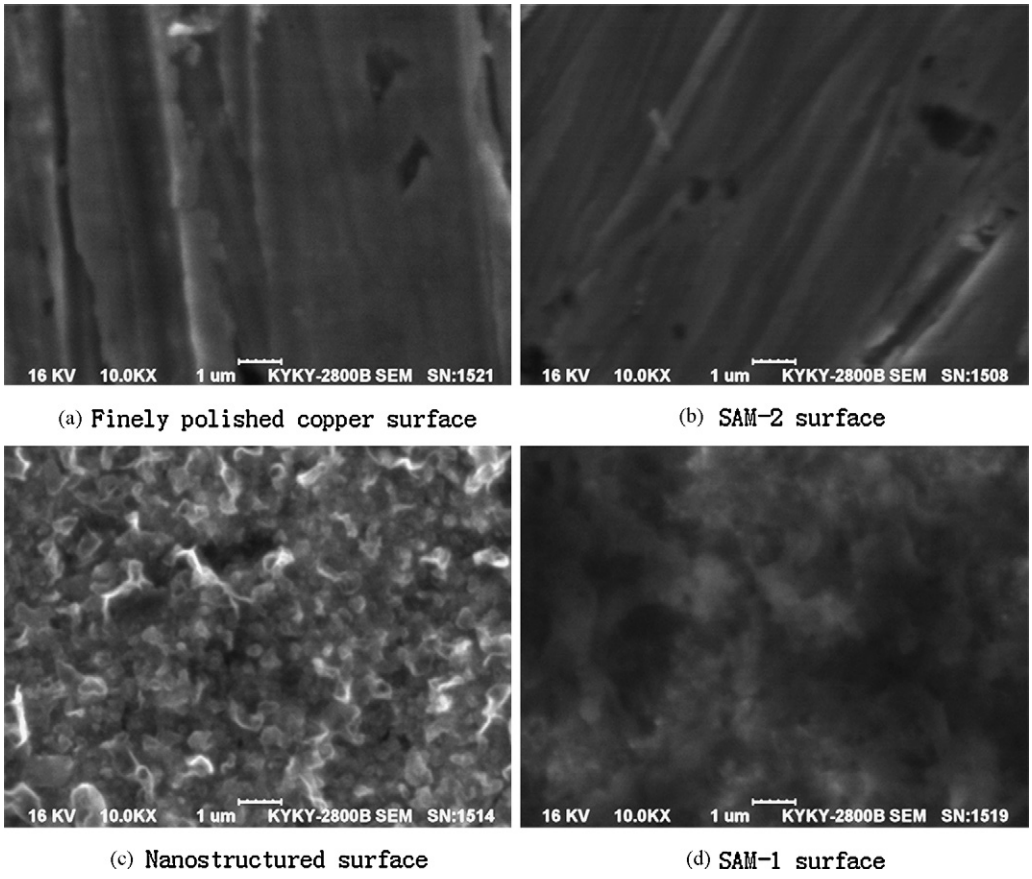

Fig. 4. SEM images of (a) finely polished copper surface; (b) SAM-2 surface; (c) nanostructured surface (copper substrate after oxidation and etching), (d) SAM-1 surface.

surfaces, respectively. Although the SAM-1 surface is much more hydrophobic than the SAM-2 surface, experimental data revealed that the superhydrophobic SAM-1 surface with nanostructures did not improve the heat-transfer performance much more during the DWC process. It is likely due to the interfacial interaction between the condensate and the condensing surface resulted from the different configurations of the SAM coated surfaces as discussed above in Section 4.3.

As shown in Fig. 4, SAM-1 coated surface is oxided and etched as many fractal-like nanostructures. In the air circumstance, the contacting surface between the water droplet and the SAM-1 coated solid surface is exactly a composite interface of solid-air-liquid, comprising the hydrophobic surface coated with SAM and the air filling in the voids of the surface. The surface free energy is smaller than that of SAM-2 coated surface. And the liquid–solid surface free energy difference for SAM-1 coated surface is higher than

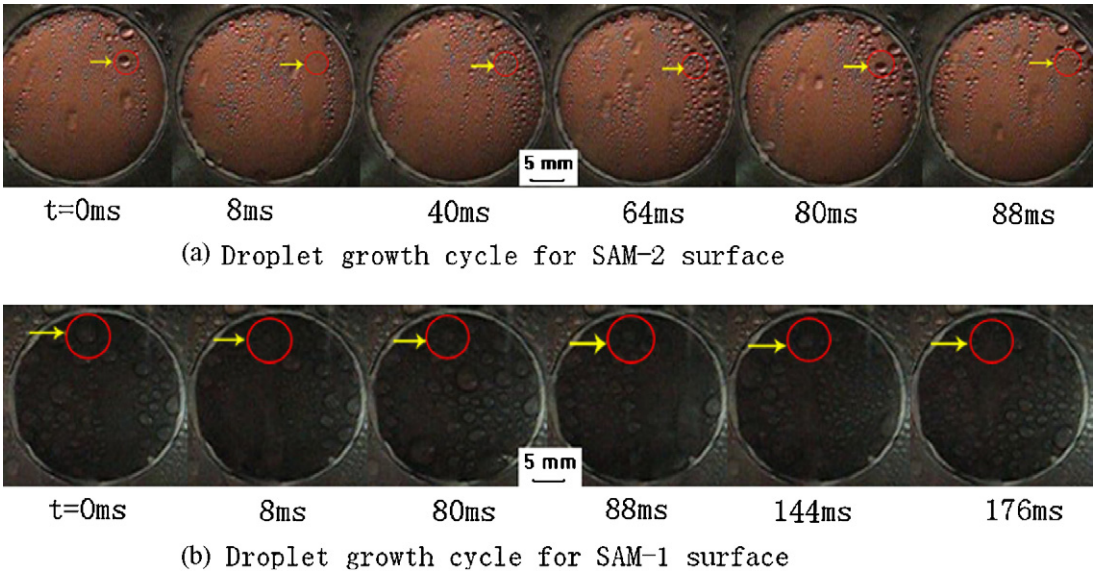

Fig. 5. Droplet growth cycle during DWC on (a) SAM-2 surface, (b) SAM-1 surface (Sub-cooling temperature: ΔT = 3–5 K, Pressure: atmospheric pressure).

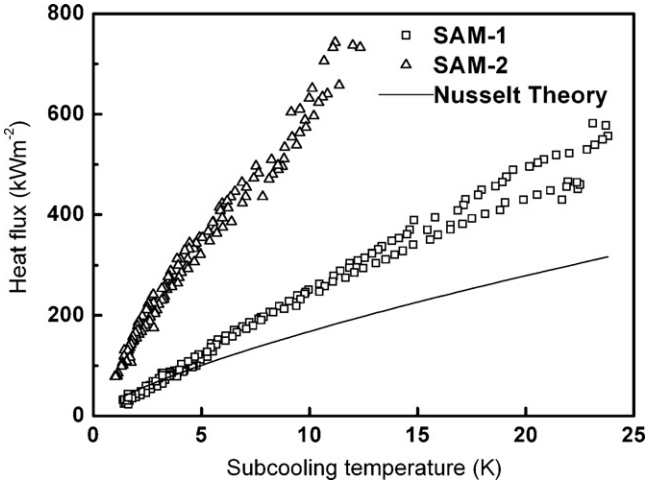

Fig. 6. DWC heat-transfer characteristics on SAM-1 and SAM-2 coated surfaces.

that of SAM-2, which results in a larger apparent contact angle. Accordingly, according to modified Cassie–Baxter model, the SAM-1 surface would show a better performance of superhydrophobicity and a larger apparent contact angle in the air-steam environment. However, in steam condensation process, usually assuming that condensate filled the cavities of SAM-1 coated surface without air. This implies that the DWC takes place at a composite surface, comprising SAM-1 coated surface and condensate. Therefore, the apparent surface free energy of the SAM-1 coated condensing surface is greater than that of SAM-2, which results in a smaller liquid–solid surface free energy difference and a larger contact angle hysteresis. Consequently, the DWC heat-transfer coefficients for SAM-1 surface are lower than those of SAM-2. Wier and McCarthy [29] also reported that the dynamic contact angles decrease substantially after steam condensed on a superhydrophobic surface.

As the contact angle hystersis is larger for nanostructured SAM-1 surface, the droplet departure diameter on the nanostructured surface during dropwise condensation is larger than that on SAM-2 surface, due to the adhesion effect of the hierarchical micro- and nano-structures. As shown in Fig. 5, the departure diameter and the growth cycle of the droplets on SAM-1 surface both are larger than those on SAM-2 surface. These also lead to a decrease in the heat-transfer performance for the SAM-1 nanostructured surface.

6. Conclusions

The oxidation and etching treatment were applied to construct nanostructures on the copper surface. Superhydrophobic and hydrophobic surface were prepared with self-assembled monolayers (SAM) coatings of n-octadecyl mercaptan on copper substrate with and without nanostructure to promote DWC. Conclusions were drawn from the results:

(1) The experimental data show that the superhydrophobic surface with nanostructures shows a better performance of superhydrophobicity and a larger apparent contact angle in the air atmosphere, but it can not improve the heat-transfer performance much more for the DWC process. The mirror-polished surface SAM-2 shows a better performance than the SAM-1 surface with nanostructures.
(2) The interfacial interaction between the condensate and the condensing surface is an important factor for the DWC heat-transfer. The contacting surface between the droplet and the superhydrophobic surface with nanostructures is typically a composite solid-condensate-liquid interface during the steam condensation process and resulting in a decrease in the liquid-solid surface free energy difference between the condensate and the condensing surface, and then decrease in the heat-transfer performance of DWC on superhydrophobic surfaces.
(3) An increase of the droplet departure diameter and a lower departure frequency, for a larger contact angle hystersis on the nanostructured surface during the DWC process, also results in a decrease in the heat-transfer performance of the SAM-1 nanostructured surface.
(4) The interface effect, such as liquid-solid free energy difference and the contact angle hysteresis, influences the heat-transfer performance much more.
(5) The experimental data demonstrated that the surface free energy and nanostructures affects the condensation heat-transfer significantly. The interaction effect and mechanism remain to be studied.

Acknowledgements

The authors are grateful to the financial supports by the National Natural Science Foundation of China (No. 50776012), Program for New Century Excellent Talents in University (NCET-05-0280), and Fund for Excellent Young Teachers of DUT (Lan Zhong).

References

[1] E. Schmidt, W. Schurig, W. Sellschopp, Versuche, Über die kondensation in film-und tropfenform, Technol. Mech. Thermodyn. (Forsch. Ing. Wes.) 1 (1930) 53–63.
[2] J.W. Rose, Dropwsie condensation theory and experiment: a review, Proc. Inst. Eng. Part A: J. Power Energy. 216 (2001) 115–128.
[3] X.H. Ma, J.W. Rose, D.Q. Xu, J.F. Lin, B.X. Wang, Advances in dropwsie condensation heat transfer: Chinese research, Chem. Eng. J. 78 (2000) 87–93.
[4] X.H. Ma, J.B. Chen, D.Q. Xu, J.F. Lin, C.S. Ren, Z.H. Long, Influence of processing conditions of polymer film on dropwise condensation heat transfer, Int. J. Heat Mass Transfer. 45 (16) (2002) 3405–3411.
[5] S. Vemuri, K.J. Kim, An experimental and theoretical study on the concept of dropwise condensation, Int. J. Heat Mass Transfer. 49 (2006) 649–657.
[6] R. Marek, J. Straub, Analysis of the evaporation coefficient and the condensation coefficient of water, Int. J. Heat Mass Transfer. 44 (2001) 39–53.
[7] X.H. Ma, L. Wang, J.B. Chen, X.B. Zhou, J.M. An, Condensation heat transfer of steam on vertical dropwise and filmwise coexisting surfaces with a thick organic film promoting mode, Exp. Heat Transfer. 16 (2003) 239–253.
[8] X.H. Ma, X.F. Chen, Analysis of effect of solid-liquid contact angle on heat transfer enhancement of filmwise condensation, J. Chem. Ind. Eng. (China) 54 (2003) 850–853.
[9] X.D. Wang, X.F. Peng, J.C. Min, T. Liu, Hysteresis of contact angle at liquid solid interface, Chinese J. Basic Sci. Eng. 9 (4) (2001) 333–343.
[10] S. Hatamiya, H. Tanaka, Dropwise condensation of steam at low pressures, Int. J. Heat Mass Transfer. 30 (1987) 497–507.
[11] Y.L. Lee, T.H. Fang, Y.M. Yang, J.R. Maa, The enhancement of dropwise condensation by wettability modification of solid surface, Int. Commun. Heat Mass Transfer. 25 (1998) 1095–1103.
[12] P.J. Marto, D.J. Looney, J.W. Rose, A. Wanniarachchi, Evaluation of organic coatings for the promotion of dropwise condensation of steam, Int. J. Heat Mass Transfer. 29 (1986) 1109–1117.
[13] K.M. Holden, A. Wanniarachchi, P.J. Marto, D.H. Boone, J.W. Rose, The use of organic coatings to promote dropwise condensation of steam, ASME J. Heat Transfer. 109 (1987) 768–774.
[14] T. Haraguchi, R. Shimada, S. Kumagai, T. Takeyama, The effect of polyvinylidene chloride coating thickness on promotion of dropwise steam condensation, Int. J. Heat Mass Transfer. 34 (12) (1991) 3047–3054.
[15] X.H. Ma, D.Q. Xu, J.F. Lin, Dropwise condensation on super thin polymer surface, J. Chem. Ind. Eng. (China) 44 (2) (1993) 165–170.
[16] Q. Zhao, D. Zhang, J.F. Lin, Surface material with dropwise condensation made by ion implantation technology, Int. J. Heat Mass Transfer. 34 (11) (1991) 2833–2835.
[17] X.H. Ma, J.B. Chen, D.Q. Xu, J.F. Lin, C.S. Ren, Z.H. Long, Influence of processing conditions of polymer film on dropwise condensation heat transfer, Int. J. Heat Mass Transfer. 45 (2002) 3405–3411.
[18] A.K. Das, H.P. Kilty, P.J. Marto, B.G. Andeen, A. Kumar, The use of an organic self-assembled monolayer coating to promote dropwise condensation of steam on horizontal tubes, ASME J. Heat Transfer. 122 (2000) 278–286.
[19] M. Izumi, S. Kumagai, R. Shimada, N. Yamakawa, Heat transfer enhancement of dropwise condensation on a vertical surface with round shaped grooves, Exp. Therm. Fluid Sci. 28 (2004) 243–248.

[20] X.H. Ma, X.F. Chen, T. Bai, J.B. Chen, A new mechanism for condensation heat transfer enhancement: effect of the surface free energy difference of condensate and solid surface, J. Enhanced Heat Transfer. 11 (4) (2004) 257–265.
[21] Z. Lan, Effect of the interfacial interaction on condensation heat transfer, Doctor's Dissertation, Dalian University of Teehnology 2006.
[22] A.W. Neumann, A.H. Abdelmessih, A. Hameed, The role of contact angles and contact angle hysteresis in dropwise condensation heat transfer, Int. J. Heat Mass Transfer. 21 (7) (1978) 947–953.
[23] C.W. Extrand, Model for contact angle and hysteresis on rough and ultraphobic surfaces, Langmuir 18 (2002) 7991–7999.
[24] J. Kijlstra, K. Reihs, A. Klami, Roughness and topology of ultrahydrophobic surfaces, Colloid Surf. A 206 (2002) 521–529.
[25] Y.C. Jung, B. Bhushan, Contact angle, adhesion and friction properties of micro- and nanopatterned polymers for superhydrophobicity, Nanotechnology 17 (2006) 4970–4980.
[26] C.H. Chen, Q.J. Cai, C. Tsai, C.L. Chen, Dropwise condensation on superhydrophobic surfaces with two-tier roughness, Appl. Phys. Lett. 90 (2007) 173108.
[27] A.B. Cassie, S. Baxter, Wettability of porous surfaces, Trans. Faraday Soc. 40 (1944) 546–551.
[28] M. Nosonovsky, B. Bhushan, Hierarchical roughness makes superhydrophobic states stable, Microelectron. Eng. 84 (2007) 382–386.
[29] K.A. Wier, T.J. McCarthy, Condensation on ultrahydrophobic surfaces and its effect on droplet mobility: ultrahydrophobic surfaces are not always water repellant, Langmuir 22 (2006) 2433–2436.